Scattering angle dependence of the surface excitation probability in reflection electron energy loss spectra

Wolfgang S. M. Werner
Institut für Allgemeine Physik, Vienna University of Technology, Wiedner Hauptstraße 8–10, A 1040 Vienna, Austria

Christoph Eisenmenger-Sittner
Institut für Angewandte und Technische Physik, Vienna University of Technology, Wiedner Hauptstraße 8–10, A 1040 Vienna, Austria

Josef Zemek and Petr Jiricek
Institute of Physics, Academy of Sciences of the Czech Republic, Na Slovance 2, 182 21 Prague 8 Czech Republic
(Received 12 December 2002; published 28 April 2003)

Reflection electron energy loss spectra (REELS) of medium energy electrons backreflected from a tungsten surface were measured. The incident and exit angles were varied over a large angular range keeping the scattering angle fixed. Two scattering geometries were studied corresponding to situations where the distribution of pathlengths of the electrons near the surface are significantly different. The spectra were decomposed into contributions of surface and volume excitations. It was found that the surface excitation probability depends not only on the incident and emission angle, but also on the scattering angle. This implies that elastic deflections in the surface scattering zone play a significant role in an energy loss experiment. Thus, the path of the reflected electrons crossing the surface scattering zone is not generally rectilinear. In consequence, plural surface scattering is not governed by the Poisson stochastic process.

DOI: 10.1103/PhysRevB.67.155412 PACS number(s): 73.20.Mf, 68.49.−h, 79.20.−m, 82.80.Pv

I. INTRODUCTION

The strong electron-solid interaction in surface electron spectroscopies such as Auger-electron spectroscopy (AES) and photoelectron spectroscopy (XPS) is responsible for the high surface sensitivity of these techniques. Therefore a detailed understanding of the processes relevant for the electron-solid interaction is a prerequisite for quantitative spectrum interpretation. These processes comprise elastic scattering as well as bulk (volume) and surface inelastic scattering. The surface modes of the inelastic excitation have a lowered resonance frequency and are orthogonal to the volume modes. In other words, the volume modes are partly depolarized by the surface charge leading to a decrease in the volume modes near the boundary. This so-called *begrenzungs* effect was predicted almost half a century ago[1] and was recently identified in reflection electron energy loss spectra (REELS) spectra of some nearly free electron (NFE) materials.[2,3]

Several models for surface excitations have been put forward in the past decades.[1,4–12] Generally, both the magnitude of the surface excitation probability as well as the distribution of energy losses in a surface excitation depend in a complex manner on the direction of surface crossing, the depth below the surface and the energy lost in a surface scattering process. Furthermore, significant interference effects occur for electrons backscattered at a given depth that depend on the incident and outgoing direction as well as on the depth.[7,10,11,13] Interference effects introduce oscillations in the depth dependence of the surface excitation probability. However, Vicanek showed that although interference effects may be strong for an individual trajectory, they cancel out to a high degree when a large number of trajectories is considered.[11]

A further simplification was proposed by Chen[14] who observed that the average penetration depth in electron spectroscopy is large compared to the depth range where surface excitations play a significant role. Therefore it was proposed to describe the influence of surface excitations in terms of a single parameter, the surface excitation parameter (SEP). This quantity represents the average number of surface excitations and the associated distribution of energy lossess in a single surface crossing along a certain direction. The above definition of the SEP pertains to electrons crossing the surface scattering zone along a rectilinear path. For a reflection electron energy loss spectrum this implies that the SEP depends on the incoming and outgoing direction only and is independent of the scattering angle.

It has been known for a long time, however, that a REELS spectrum also depends on the scattering angle, both in shape and magnitude.[3,15,16] The reason is that the path length distribution of the backreflected electrons inside the solid is not necessarily a monotonically decaying function of the pathlength but depends quite sensitively on the scattering geometry. The question then arises whether the surface excitation probability also depends on the scattering angle. This question is studied in the present work. It is found that the magnitude of the surface excitation probability measured in a REELS experiment indeed depends on the scattering angle and is therefore not equal to the SEP as defined above. On the other hand, the shape of the distribution of energy losses in a single surface excitation agrees remarkably well with the theory of Tung and co-workers.[9]

II. BULK SCATTERING AND SELECTION OF SCATTERING GEOMETRIES

The aim of the present work is to study the influence of the distribution of pathlengths traveled by reflected electrons

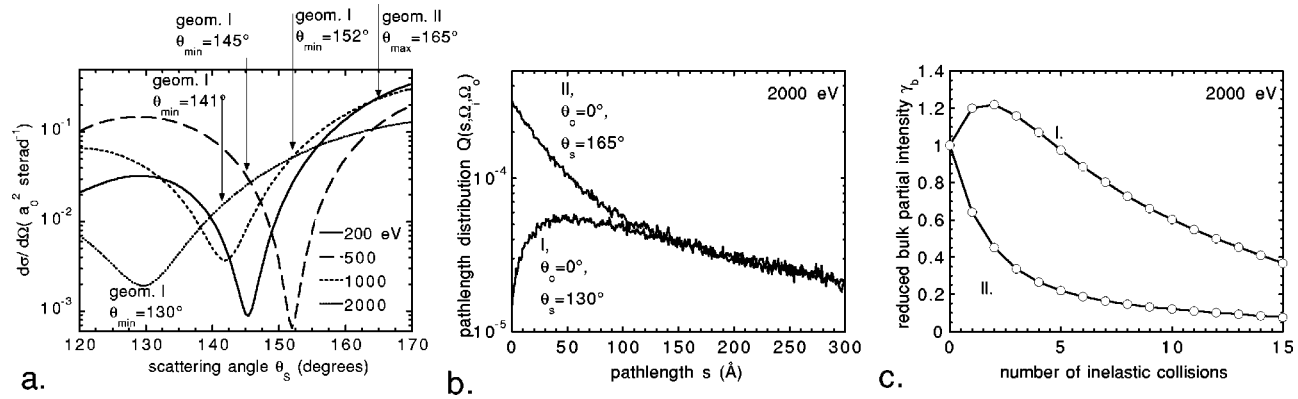

FIG. 1. (a) Differential elastic scattering cross section of electrons of several energies in tungsten. The portion of the cross section shown comprises the relevant scattering geometries used in the experiments described in the present work. For each energy scattering angles corresponding to a minimum and a maximum (geometries I and II) were used. (b) path length distribution for reflection of 2000 eV electrons in tungsten for geometries I and II for normal electron exit. (c) Reduced bulk partial intensities $\gamma_{n_b}=C_{n_b}/C_{n_b=0}$ for the pathlength distributions displayed in (b).

in the vicinity of the surface on the surface excitation probability. The pathlength distribution is entirely governed by the elastic electron-solid interaction if the dynamical forces acting upon the probing particles in the course of the inelastic interaction can be neglected. For energies above $\sim$200 eV this condition is generally met.[8] Furthermore the deflections suffered by the projectiles due to momentum transfers in an inelastic collision can be generally neglected due to the large mass difference between the projectile and its collision partner, the solid.[17] Then, the pathlength distribution is entirely governed by the elastic scattering cross section.

Figure 1(a) shows the portion of the scattering cross section of W relevant to our experiments. This quantity was calculated with the partial wave expansion method[18] using free atomic Thomas-Fermi-Dirac potentials.[19] The scattering angles used in the experiments are indicated for each energy. The two different scattering geometries used for each energy will be denoted by geometry I (for a minimum in the cross section) and geometry II (for the case corresponding to a maximum in the cross section) in the following. Geometry II was chosen to be identical for all energies with a scattering angle of $\theta_s=165°$ the scattering angles chosen for geometry I vary with the incident energy and are listed in Table I.

TABLE I. Parameters used in the simulation of the partial intensities with the models discussed in the text. The scattering angle chosen for each energy for geometry I is given by θ_s, λ_e is the elastic mean free path (Refs. 18,19), the inelastic mean free path was taken from Ref. 34, the width of the surface scattering layer v/ω_s was calculated in the jellium model (see text).

E (eV)	θ_s (deg)	λ_e (Å)	λ_i^{TPP} (Å)	v/ω_s (Å)
200	145	2.2	5.7	2.1
500	152	3.9	9.4	3.4
1000	141	5.3	15.1	4.8
2000	130	7.2	25.3	6.8

The distribution of pathlengths traveled by the electrons for these geometries was modeled by means of a Monte Carlo (MC) calculation in which only elastic scattering is taken into account.[16,17] The resulting distribution of pathlengths s traveled in the solid, $Q(s,\vec{\Omega}_i,\vec{\Omega}_o)$ is shown for normal emission for 2000 eV electrons in Fig. 1(b). Here $(\vec{\Omega}_i,\vec{\Omega}_o)$ denote the incoming and outgoing direction of motion of the projectile. A significant difference between the two pathlength distributions is seen: For the geometry corresponding to a maximum in the cross section (geometry II), a monotonically decaying pathlength distribution is obtained. For the geometry corresponding to a minimum in the cross section (geometry I), a rather steep increase is observed near the surface as well as a maximum at greater depth. The difference in the behavior for the two geometries has a clear physical explanation:[15,16] For geometry II the likelihood that an electron experiences exactly the deflection needed to reach the detector in a single elastic collision is large since the elastic scattering cross section is large for this scattering geometry. For geometry I the particle has to participate in more elastic events before the net deflection matches the detection geometry. Consequently, the pathlength traveled inside the solid will be longer.

For a given pathlength distribution, the number of electrons reaching the detector after participating in n_b collisions, the so−called bulk partial intensities C_{n_b} are given by[17]

$$C_{n_b}=\int_0^\infty Q(s)\left(\frac{s}{\lambda_{i,b}}\right)^{n_b}\frac{e^{-(s/\lambda_{i,b})}}{n_b!}ds, \qquad (1)$$

where $\lambda_{i,b}$ is the bulk inelastic mean free path (IMFP). These quantities are shown in Fig. 1(c) for 2000 eV for the pathlength distribution shown in Fig. 1(b). Obviously, the sequence of partial intensities determines the shape of the loss features of a REELS spectrum. It is therefore expected that for the geometry II the intensity of the loss spectrum decreases rapidly with the energy loss, while this decrease is much less pronounced for geometry I.

It should be noted that the pronounced differences in the pathlength distribution, seen in Fig. 1(b) for different scattering geometries, do not only occur for materials with strong oscillations in the plot of the differential elastic-scattering cross section as a function of the scattering angle (high atomic numbers). For light materials, where the path length distribution does not exhibit a pronounced dependence on the scattering geometry, changes in the pathlength distribution similar to those in Fig. 1(b) are observed as a function of the scattering energy.[3] This implies that it is generally necessary to account in detail for the elastic interaction when quantitatively interpreting reflection electron energy loss spectra.

III. SURFACE EXCITATIONS

As already pointed out in the Introduction, a coupling of surface and bulk excitations exists that is often refered to as *begrenzungs* effect. Therefore the distinction between surface and bulk excitations is essentially artificial. Nonetheless, a clear definition of terms is indispensable for a proper understanding of the physics relevant for the energy loss process. By ''bulk excitations'' we will denote any energy loss phenomenon occuring in an infinite medium without any boundary. Likewise, any change in the excitation probability due to the presence of a solid-vacuum boundary will be referred to as ''surface excitation.''

Generally two aspects of the energy loss process can be distinguished (and treated separately): the integral excitation intensity and the energy fluctuations associated with it. Arista[8] has shown that for the integral collision statistics, a single plasmon resonance model with appropriately chosen parameters is accurate. The distinction between energy loss fluctuations and collision statistics also forms the theoretical basis for describing an electron spectrum in the so-called partial intensity approach. In this approach, the number of electrons reaching the detector after participating in a given number of surface (n_s) and bulk (n_b) excitations is described by the partial intensities C_{n_b,n_s},[17] while energy fluctuations for a given number of collisions are described by the associated partial energy (loss) distributions.

In a situation were both bulk and surface excitations are relevant, the partial intensities are often assumed to be of the form[3,9,14,17,20–23]

$$C_{n_b,n_s}=C_{n_b}C_{n_s}. \tag{2}$$

Equation (2) states that the partial intensities for bulk and surface excitations are uncorrelated.[2,20,21] The physical reason for this assumption is closely related to the elastic scattering characteristics of medium energy electrons in solids. This is illustrated in Fig. 2(a) that shows a trajectory of a 200 eV electron backscattered from a W surface calculated with the MC method. The open circles indicate the location of an elastic process; inelastic scattering is not considered in the simulation.

In the lower panel of Fig. 2 the stopping power for the different loss mechanisms is illustrated on the same depth scale. It comprises the three terms addressed above: the pure

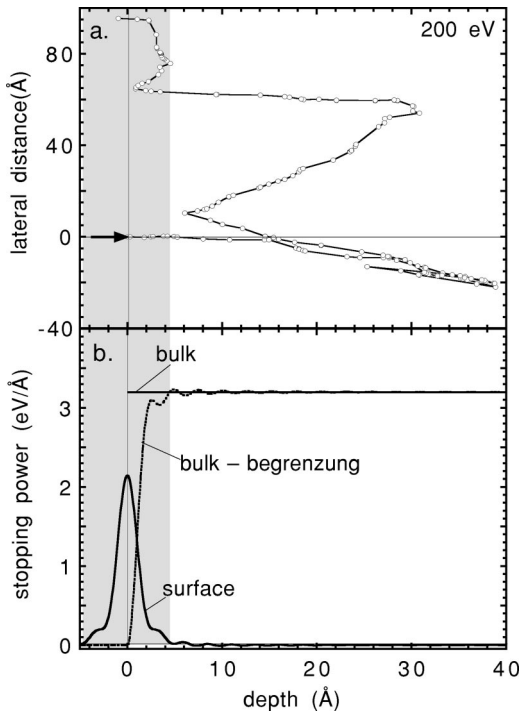

FIG. 2. (a) Trajectory of a 200 eV electron reflected from a tungsten surface simulated by the Monte Carlo (MC) method. Only elastic collisions, represented by the open circles, were considered in the simulation. (b) Depth dependence of the bulk and surface stopping power calculated with Arista's model (Ref. 8) for a tungsten surface in the jellium model. The solid line labeled ''bulk:'' bulk excitations; the solid line labeled ''surface:'' the pure surface term in Eq. (3); the dashed line is the superposition of the bulk and *begrenzungsterm* and indicates the depth range where the intensity of bulk excitations is decreased due to the depolarization by the surface charge.

surface term, the begrenzungs correction of the bulk stopping power due to the depolarization by the surface charges in the vicinity of the surface and the bulk term. These terms are approximately given by the expressions[5,6,8,11]

$$\left(\frac{dT}{ds}\right)_{surf}=\frac{e^2\omega_s^2}{v^2}K_0\left(\frac{2\omega_s|z|}{v}\right),$$

$$\left(\frac{dT}{ds}\right)_{begr}=-\frac{e^2\omega_b^2}{v^2}K_0\left(\frac{2\omega_b z}{v}\right),$$

$$\left(\frac{dT}{ds}\right)_{bulk}=\frac{e^2\omega_b^2}{v^2}\ln\frac{k_c v}{\omega_b}. \tag{3}$$

Here v is the electron speed, e^2 is the elementary charge squared, z is the distance above or below the surface, k_c is a cutoff wave vector and K_0 is the modified Bessel function. Equation (3) is based on the jellium model describing the dielectric response of the solid in terms of three parameters, the bulk plasmon energy $\hbar\omega_b$, a damping constant γ and the cutoff frequency k_c. The surface plasmon frequency is given by $\omega_s=\omega_b/\sqrt{2}$. We derived a value of $\hbar\omega_b=25.8$ eV for the

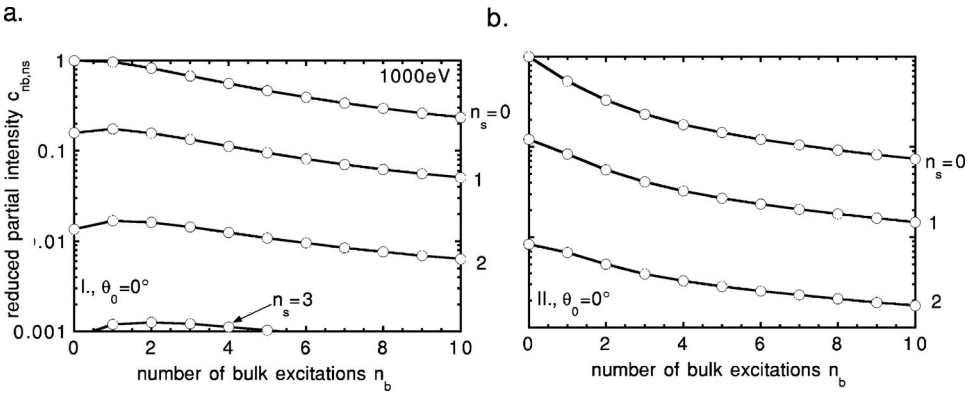

FIG. 3. Reduced partial intensities $c_{n_b,n_s}=C_{n_b,n_s}/C_{n_b=0,n_s=0}$ for reflection of 1000 eV electrons calculated with Arista's model (Ref. 8) for tungsten jellium at normal electron exit. (a) Geometry I. (b) Geometry II.

bulk plasmon frequency from optical data,[24] and used a value of $k_c=0.5/a_0$ for the cutoff wave vector, where a_0 is the first Bohr radius.

The influence of the boundary is seen to decay approximately exponentially with the depth both inside and outside the solid-vacuum interface. The decay length of this depth dependence is approximately given by v/ω_s. On the other hand, bulk excitations only occur inside the solid. The intensity of the begrenzungs correction is seen to decrease with the depth from the surface and essentially vanishes for depths greatly exceeding v/ω_s.

It is seen in Fig. 2(a) that the average distance between two elastic processes (the elastic mean free path, λ_e) is of the order of the thickness of the surface scattering zone (see also Table I). Furthermore, the majority of the scattering processes give rise to a deflection over a small angle while the average distance between large angle processes is even much larger than the elastic mean free path. Therefore, when the condition

$$\lambda_e \gtrsim v/\omega_s \tag{4}$$

is fullfilled, the majority of all electrons approximately cross the surface scattering zone along the same rectilinear path determined by the considered scattering geometry. Note, however, that the trajectory displayed in Fig. 2(a) fullfills this condition for the ingoing surface crossing, but also provides a clear counterexample for the outgoing surface crossing. If all electrons travel along the same path through the surface scattering layer, then the surface excitation probability will be the same for all of them for an *arbitrary* depth dependence of the surface excitation probability. In this case Eq. (2) is obviously strictly correct. The above also immediately implies that multiple surface excitations are governed by Poisson statistics:

$$C_{n_s}=\langle n_s\rangle^{n_s}\exp(-\langle n_s\rangle)/n_s! \tag{5}$$

when $\langle n_s\rangle$ is the average number of surface excitations in a single surface crossing and the surface partial intensity C_{n_s} represents the probability for experiencing n_s surface excitations for a single surface crossing. The quantity $\langle n_s\rangle$ in Eq. (5) exactly corresponds to the surface excitation parameter as defined by Chen[14] if the path of the surface crossing is rectilinear. Then the SEP is approximately given by[1,14]

$$\langle n_s(\theta)\rangle=\frac{a}{\sqrt{E}\cos\theta} \tag{6}$$

where θ is the polar angle of surface crossing. For nearly free electron materials one has $a=a_{\mathrm{NFE}}=(\pi^2e^2/32a_0)^{1/2}=2.89\ \mathrm{eV}^{1/2}$. For the group of materials Al, Cu, Ag, Au, Fe, Si and GaAs the same functional form holds with $0.75\lesssim a/a_{\mathrm{NFE}}\lesssim 1.42$.[25]

Results of model calculations for the partial intensities on the basis of Arista's results [see Fig. 2(b)] and a realistic elastic scattering cross section (see Fig. 1) are shown in Fig. 3 for 1000 eV for the geometries I and II. Here the assumption Eq. (2) was not taken as a starting point; on the contrary, these simulations are performed to test this assumption. Although these results are approximate (see Ref. 8), they allow us to draw some qualitative conclusions. Again a significant difference is observed between the two geometries. Note, however, that in both cases the curves for different values of n_s are approximately parallel on a logarithmic scale, implying that the assumption Eq. (2) is justified to a high degree. Only for $n_b\sim 0$ are the curves not exactly parallel. Furthermore, it is seen that although the curves are approximately parallel, the numerical factor between two neighboring curves varies with n_s. This means that the surface partial intensities do not follow a Poisson distribution as per Eq. (5). The reason is that elastic scattering does play a significant role in the surface crossing. This also implies that the surface excitation probability is not generally equal to the surface excitation parameter, the latter quantity being defined for rectilinear surface crossing. It is to be noted that the observed correlation between the surface and bulk partial intensities is rather weak and, moreover, that plural surface scattering ($n_s\gtrsim 2$) only contributes very slightly to the expected total intensity and can therefore often be neglected. Under these conditions, the REELS analysis procedure presented in the next section retains its validity in spite of the fact that Eqs. (2) and (5) are not strictly valid.

IV. DETERMINATION OF THE SURFACE EXCITATION PROBABILITY FROM REELS

For completeness, a synopsis of the method to extract the differential surface excitation probability from experimental spectra[2] is given below. This procedure follows the definition discussed above that all phenomena in the loss spectra

caused by the presence of the boundary are regarded as surface excitations. The basic assumption underlying this procedure is that bulk and surface excitations are uncorrelated [Eq. (2)]. It provides the differential surface excitation probability (incoming as well as outgoing) in absolute units in two steps:[2,3] (1) elimination of multiple bulk scattering and (2) retrieval of the differential surface excitation probability from the resulting spectrum.

Removal of multiple bulk scattering can be accomplished by iterative application of the formula[17,26,27]

$$Y_{k+1}(E)=Y_k(E)-q_{k+1}\int Y_k(E+T)L_{k+1}(T)dT, \quad (7)$$

where Y_k is the spectrum from which the contribution of k-fold scattering has been eliminated. The coefficients q_k are functions of the reduced bulk partial intensities $\gamma_{n_b}=C_{n_b}/C_{n_b=0}$ given by

$$q_1=\gamma_1,$$

$$q_2=\gamma_2-q_1q_1,$$

$$q_3=\gamma_3-q_1q_2-q_1q_1q_1,$$

$$q_4=\gamma_4-q_1q_3-q_2q_2-q_1q_1q_2-q_1q_1q_1q_1, \ldots . \quad (8)$$

The subscripts of the coefficients q_k in Eq. (8) are the partitions of the natural numbers.[28] The quantities $L_k(T)$ are the partial loss distributions in a volume excitation

$$L_k(T)=\int L_{k-1}(T-T')w_b(T')dT', \quad (9)$$

where $w_b(T)$ is the normalized differential mean free path for volume scattering, i.e., the distribution of energy losses in a single bulk excitation.

The second step can be expressed in terms of the loss spectrum $Y_L^1(T)$ that is obtained by eliminating the elastic peak from the spectrum obtained after the first step, normalized with the area of the elastic peak. Denoting the $(k-1)$-fold self-convolution of the loss spectrum by $Y_L^k(T)$, the loss distribution $W_s(T)$ is found in absolute units as[26]

$$W_s(T)=\sum_{k=1}^{N}\frac{(-1)^{k+1}}{k}Y_L^k(T), \quad (10)$$

where N has to be chosen large enough to attain convergence. Obviously, the retrieved distribution in a REELS experiment is representative for the combined effect of the incoming and outgoing surface crossing. The total surface excitation probability [the area of $W_s(T)$] is therefore equal to $\langle n_s(\theta_i)\rangle+\langle n_s(\theta_o)\rangle$. Note that the second step in the present method is completely equivalent to the retrieval procedure for the bulk inelastic loss distribution from energy loss spectra in the transmission electron microscope.[29,30]

V. EXPERIMENTAL

Tungsten samples were prepared by sputter depositing $\sim 0.5\ \mu$m W on pieces of a Si wafer under high vacuum conditions. Auger electron spectra were taken on a VG Microlab 310F to verify that the W layer formed in this way was free of any oxygen contamination. Furthermore, secondary electron images taken with a ~ 10 nm spot size field emission electron gun revealed that the samples were smooth on this lateral scale.

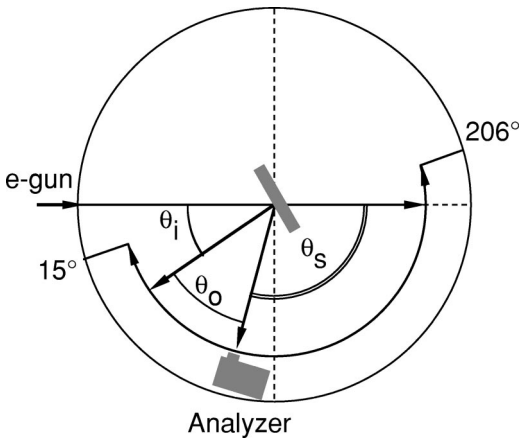

FIG. 4. Schematic illustration of the experimental geometry. The angles of incidence (θ_i) and exit (θ_o) as well as the scattering angle (θ_s) are indicated.

REELS and XPS measurements were performed using an ADES-400 angular-resolved photoelectron spectrometer (VG Scientific, UK) equipped with an electron gun (Varian, Model 981-2454) and a twin anode x-ray source with the standard Al/Mg anodes and with a hemispherical electron energy analyzer. The geometry of the experimental setup is illustrated in Fig. 4. The analyzer lies in the plane of incidence and can be rotated around the sample in the range of analyzer angles between 15° and 206°. In addition, the sample surface normal can be rotated by 360° in the plane of incidence. The half-cone acceptance angle of the analyzer was set to 4.1°.

REELS spectra were measured for electron energies E_0 of 200, 500, 1000, and 2000 eV for energy losses in the range 0–100 eV and a pass energy of 30 eV. For each energy, the emission angular distribution ($\theta_o=0°,15°,30°,45°,60°,75°$) was measured for two different values of the scattering angle corresponding to a maximum and a minimum in the elastic scattering cross section (see Fig. 1).

VI. RESULTS AND DISCUSSION

The REELS spectra for geometry I and II for 1000 eV electrons for normal exit are shown in Fig. 5 by the dotted lines. It is seen that for geometry II the intensity of the loss spectrum decreases with increasing energy loss, while for geometry I the loss spectrum is almost completely flat. This is in agreement with the finding in the previous section that the pathlength distributions and partial intensities are markedly different for the two geometries. When this difference in the partial intensities is taken into account in the procedure

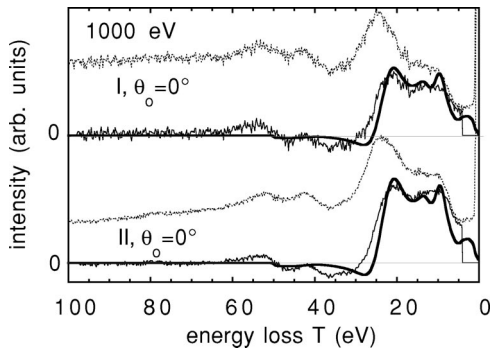

FIG. 5. REELS of 1000 eV electrons reflected from a tungsten surface for geometry I (upper panel) and geometry II (lower panel). Dotted lines: raw data; thin solid lines: differential surface excitation probability obtained with the elimination–retrieval procedure Eqs. (7)–(10); thick solid lines: single surface scattering energy loss distribution calculated with the theory in Ref. 9.

to extract the surface scattering probability [Eq. (7)], the contribution of multiple volume scattering is consistently removed. This is represented by the full thin solid line in Fig. 5. The thick solid line is an evaluation of the theory of Tung and co-workers[9] normalized to the extracted surface loss spectrum in order to facilitate comparison.

Similar results are shown for the other energies studied in the range of low energy losses (0–50 eV) in Fig. 6. In all cases the contribution of multiple bulk scattering is properly removed in spite of the fact that the shapes of the measured loss spectra are significantly different. It is also seen that the theory predicts a considerable energy dependence of the shape of the surface excitation probability. For 200 eV, the peak in the differential surface excitation probability at $\sim$10 eV is dominating while the peak at around 20 eV is slighty less pronounced. When going to higher energies, the low energy loss peak at 10 eV decreases signficantly compared to the energy loss peak at $\sim$20 eV. These features are matched remarkably well by the experimental results. Note furthermore that theory does not predict very pronounced differences between geometry I and II. This is expected since the incidence angles are always in the range 15°–50° (off-normal) where significant differences in the differential surface excitation probability are not predicted to occur. The shape of the energy loss distribution retrieved from the experimental data follows this trend. On the other hand, the raw data reveal a significant difference for the two geometries: for geometry II the ratio of the intensity the peak at $\sim$10 eV (mainly attributable to surface excitation) and the one at $\sim$25 eV (a volume loss peak) is always larger than for geometry I. This is in agreement with the finding in Fig. 1(b) that the intensity of bulk scattering should be always larger for geometry I since the pathlength distribution has a maximum at a certain depth, while for geometry two, it decays monotonically with the pathlength.

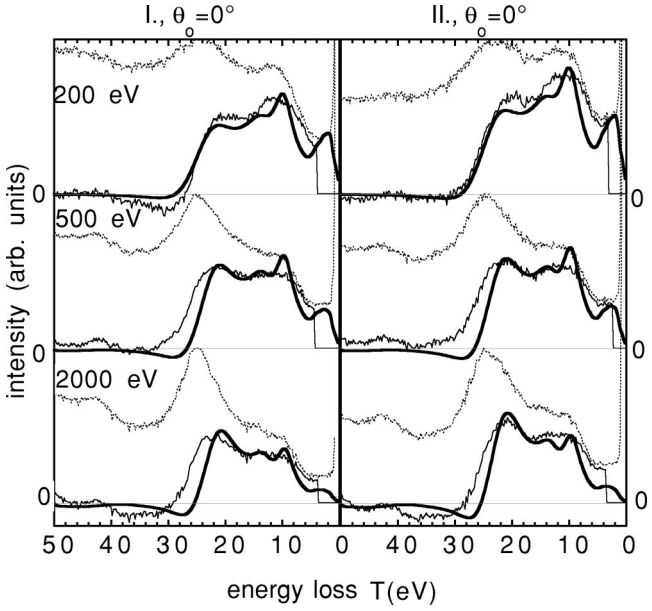

FIG. 6. Same as Fig. 5 for 200, 500, and 2000 eV for energy losses in the range 0–50 eV.

The exit angular distribution of the integrated surface excitation probability extracted from the experimental spectra is shown in Fig. 7. The left portion of this figure (open symbols and dashed lines) correspond to geometry I, the right part (closed symbols, solid lines) is for geometry II. The quantities $\varrho_{1s}=C_{n_s=1}/C_{n_s=0}$ represented by the circles are the experimental reduced single surface excitation probability normalized with the area of the elastic peak. The diamonds represent the reduced bulk partial intensities $\gamma_{1b}=C_{n_b=1}/C_{n_b=0}$ calculated with the MC method [see Fig. 1(c)]. The dashed and solid lines are the angular distribution of the SEP given by Eq. (6). Note that these curves are not symmetric with respect to the two scattering geometries since the scattering angles for geometry I were chosen differently for different geometries and are generally different to the scattering angles in geometry II. This leads to a minor difference in the surface excitation parameter for normal electron exit that is caused by the dependence of the surface excitation parameter on the incident surface crossing direction, not on the scattering angle. For larger exit angles, the surface excitation parameter given by Eq. (6) is seen to be larger for scattering geometry II.

The bulk partial intensities for one volume excitation γ_{1b} are seen to be markedly different for the two geometries in all cases since the pathlength distributions for the two cases also exhibit a qualitatively different behavior. A similar behavior, although less pronounced is seen for the surface excitation probability in an individual surface loss ϱ_{1s}. It is seen that the surface excitation probability at a given exit angle for geometry I is always larger than for geometry II. This is in sharp contradiction to the emission angle dependence predicted by Eq. (6) for rectilinear surface crossing (i.e., the surface excitation parameter) where, due to the particular choice of the scattering geometries a larger value is expected for geometry II, as indicated by the dashed and solid lines. The reason is obviously that for geometry II, by virtue of the large probability for a deflection matching the detection geometry in a single elastic collision, a larger fraction of backscattered electrons actually traverses the surface scattering zone without suffering any deflections at all. In-

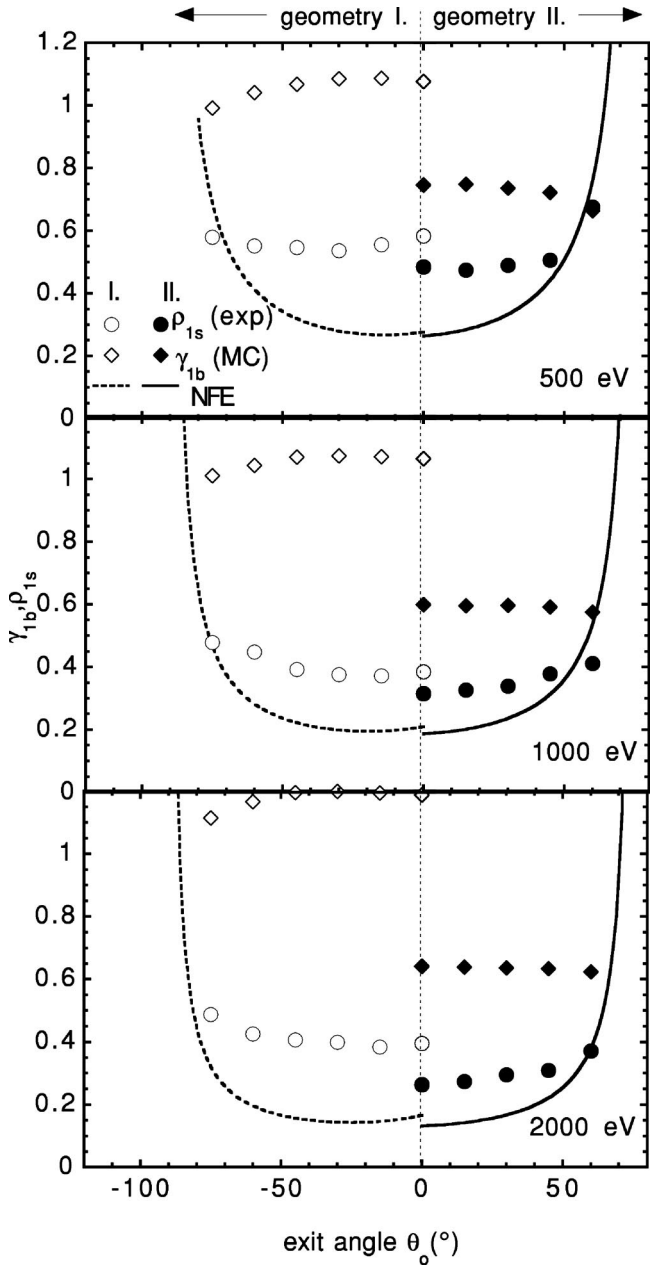

FIG. 7. Angular distribution of the reduced partial intensities for a single surface (ϱ_{1s}) and bulk (γ_{1b}) excitation for 500, 1000, and 2000 eV. Note that for a REELS experiment one has $\varrho_{1s}=\langle n_s(\theta_i)\rangle+\langle n_s(\theta_o)\rangle$, where $\langle n_s(\theta_{i,o})\rangle$ is the average number of surface excitations in a single surface crossing. Open symbols and dashed lines: geometry I; filled symbols and solid line: geometry II; circles: single surface excitation partial intensity (ϱ_{1s}) extracted from the experimental spectra; diamonds: single bulk excitation partial intensity (γ_{1b}) calculated with the MC method; lines: NFE result [Eq. (6)].

deed for geometry II, the experimental values for the surface excitation probability are in better agreement with the surface excitation parameter [Eq. (6), complete rectilinear crossing of the surface scattering zone] than for geometries I. On the other hand, for geometry I, most electrons have to travel a much longer pathlength in the solid before their direction matches the detection geometry and consequently they will be deflected several times in the surface scattering zone. In consequence they will experience a larger number of surface excitations, on the average. The scattering angle dependence of the surface excitation probability following from the difference between geometry I and II immediately allows one to draw two conclusions: (1) elastic scattering in the surface scattering zone does play a significant role in REELS experiments and, consequently, (2) the surface excitation probability measured in a REELS experiment is generally not equal to the SEP.

Therefore, it is essentially impossible to compare the experimental integrated surface excitation probability with theoretical results on an absolute scale since the latter are only given in the literature for a rectilinear surface crossing. On the other hand, the differential surface excitation probability shown in Fig. 5 and 6 is found to be in very good agreement with results based on this model. Note that the shape of the distribution of energy losses in a surface excitation is a consequence of the detailed balance of the surface and the begrenzungsterm in Eq. (3) that changes with the scattering energy.

In summary it was found that owing to elastic scattering (1) there is a minor correlation between surface and bulk excitations, (2) multiple surface excitations do not follow a Poisson distribution, and (3) the surface excitation probability is generally not equal to the SEP. The latter statement follows from the others but is mentioned separately because it can be directly observed in the experimental results in Fig. 7. The implications of these three main findings deserve to be discussed in conclusion.

First of all, the question arises whether it is at all possible to decompose surface and bulk excitations with Eqs. (7) and (10) since this procedure is based on the assumption Eqs. (2) and (5). However, the correlation in Fig. 3 is seen to be weak and, furthermore, the series in Eq. (10) converge extremely rapid since the higher order surface partial intensities $\gamma_{n_s>1}$ are very small and can usually be neglected as can be clearly seen in Fig. 3. This implies that only the upper two curves in Fig. 3 are relevant at all and these are almost perfectly parallel on a logarithmic scale, except for $n_b\sim 0$. The influence of such a weak correlation on the decomposition procedure has recently been studied by means of model calculations and was found to be insignificantly small.[21] Therefore, it is concluded that the elimination-retrieval procedure used to decompose surface and bulk excitations is applicable to the presented data for determination of the surface excitation probability.

The finding that the quantity assessed in a REELS experiment is not equal to the SEP implies that in order to meaningfully compare theory with experiment one needs to theoretically evaluate the integrated surface excitation probability along an actual path of each electron for a realistic set of trajectories. Note that the results in Fig. 3 were produced in exactly this way using a jellium model to establish the dielectric function. Indeed, when comparing the values of the reduced surface partial intensity $\varrho_{n_s=1}$ in Figs. 3(a) and 3(b) ($n_b=0,n_s=1$) it is seen that this quantity is larger for geometry I by about 25%, in perfect agreement with the result for

1000 eV in Fig. 7 for normal emission. This fact convincingly demonstrates that the larger value of the surface scattering probability for geometry I is attributable to the influence of elastic scattering in the surface scattering zone. Replacing the jellium dielectric function by a more realistic model for the dielectric response[9] should allow a direct quantitative comparison between experiment and theory. This will be the subject of further study.

It should again be emphasized here that differences in the pathlength distribution as observed for geometry I and II can occur for any element throughout the periodic table for certain combinations of the electron energy and scattering geometry. The special geometries for tungsten were only chosen here to prove the point. Such effects also occur for energies and elements that do not exhibit pronounced oscillations in the distribution of scattering angles,[3] and is therefore a general phenomenon that always needs to be properly addressed when quantitatively analyzing REELS data.

The above does not necessarily mean that the concept of the surface excitation parameter needs to be abandoned altogether. On the contrary, it is believed that in AES and XPS a refined version of this concept can be extremely useful. A fundamental difference between a reflection experiment and an emission experiment is that in the latter case, for a smooth source angular distribution, the details of the elastic cross section do not significantly influence the energy and angular distribution of the emitted intensity. This follows from the so−called generalized radiative similarity principle[31–33] that is the justification for the use of the transport approximation in the electron escape process. An important direct consequence of the validity of the transport approximation is that the emerging flux is entirely governed by a single parameter, the scattering parameter[17]

$$\chi = \frac{\lambda_i}{\lambda_{\mathrm{tr}}}, \tag{11}$$

where λ_{tr} is the transport mean free path.[17] In consequence, in AES and XPS it should be possible to define a modified surface excitation parameter that properly accounts for the surface crossing through a single additional material parameter, the scattering parameter χ.

VII. SUMMARY AND CONCLUSIONS

Spectra of electrons reflected from a tungsten surface were measured for several energies and a large range of emission angles keeping the scattering angle fixed. This was done for two specifically chosen scattering geometries pertaining to a situation where predominantly reflection at large depths (large pathlengths) and small depths (small pathlengths) contribute to the spectrum. The experimental loss spectra were decomposed into contributions attributable to surface and bulk excitations. For both geometries the normalized distribution of surface losses is in very good agreement with the theory of Tung and co-workers for the differential surface excitation parameter. A significant difference is found for the absolute surface excitation probability for the two scattering geometries. This is caused by the difference in traveled pathlengths for the two considered geometries and generally implies that the surface excitation probability measured in a REELS experiment is not equal to the surface excitation parameter. The reason is that the latter quantity is defined for penetration of the surface scattering zone along a rectilinear path. Monte Carlo calculations were performed that support this interpretation and reveal that a slight correlation between surface and bulk excitations exists that is caused by elastic scattering. The fact that elastic scattering influences the surface excitation probability also leads to the conclusion that plural surface excitations are not described by the Poisson stochastic process.

ACKNOWLEDGMENTS

This cooperation was supported by the Austrian-Czech Scientific Exchange Program KONTAKT P2002-6. Two of us (J.Z and P.J) would also like to acknowledge financial support by the Czech Academy of Sciences Grant No. GACR202/02/0237. One of us (W.S.M.W) acknowledges the support of this work by the ''Fonds zur Förderung der Wissenschaftlichen Forschung (FWF)'' (Austrian Science Foundation), through Project No. P15938-N02

[1] R. H. Ritchie, Phys. Rev. **106**, 874 (1957).
[2] W. S. M. Werner, Surf. Sci. **526/3**, L159 (2003).
[3] W. S. M. Werner, Surf. Interface Anal. **35**, 347 (2003).
[4] E. A. Stern and R. A. Ferrell, Phys. Rev. **120**, 130 (1960).
[5] P. M. Echenique and J. B. Pendry, J. Phys. C **8**, 2936 (1975).
[6] R. Nunez, P. M. Echenique, and R. H. Ritchie, J. Phys. C **13**, 4229 (1980).
[7] F. Yubero and S. Tougaard, Phys. Rev. **46**, 2486 (1992).
[8] N. R. Arista, Phys. Rev. A **49**, 1885 (1994).
[9] C. J. Tung, Y. F. Chen, C. M. Kwei, and T. L. Chou, Phys. Rev. B **49**, 16 684 (1994).
[10] C. Denton, J. B. Gervasoni, R. O. Barrachina, and N. R. Arista, Phys. Rev. A **57**, 4498 (1998).
[11] M. Vicanek, Surf. Sci. **440**, 1 (1999).
[12] K. L. Aminov and J. B. Pedersen, Phys. Rev. B **63**, 125412 (2001).
[13] A. Cohen-Simonsen, F. Yubero, and S. Tougaard, Phys. Rev. B **56**, 1612 (1997).
[14] Y. F. Chen, Surf. Sci. **345**, 213 (1996).
[15] W. S. M. Werner and M. Hayek, Surf. Interface Anal. **22**, 79 (1994).
[16] W. S. M. Werner, C. Tomastik, T. Cabela, G. Richter, and H. Störi, J. Electron Spectrosc. Relat. Phenom. **113**, 127 (2001).
[17] W. S. M. Werner, Surf. Interface Anal. **31**, 141 (2001).
[18] A. C. Yates, Comput. Phys. Commun. **2**, 175 (1971).
[19] R. A. Bonham and T. G. Strand, J. Chem. Phys. **39**, 2200 (1963).
[20] W. S. M. Werner, T. Cabela, J. Zemek, and P. Jiricek, Surf. Sci. **470**, 325 (2001).

[21] W. S. M. Werner, H. P. Winter, and H. Störi, Surf. Sci. **518**, L569 (2002).
[22] Y. F. Chen, P. Su, C. M. Kwei, and C. J. Tung, Phys. Rev. B **50**, 17 547 (1994).
[23] C. M. Kwei, C. Y. Wang, and C. J. Tung, Surf. Interface Anal. **26**, 682 (1998).
[24] E. D. Palik, *Handbook of Optical Constants of Solids* (Academic, New York, 1985).
[25] Y. F. Chen, Surf. Sci. **519**, 115 (2002).
[26] W. S. M. Werner, Surf. Interface Anal. **23**, 737 (1995).
[27] W. S. M. Werner, Phys. Rev. B **52**, 2964 (1995).
[28] S. Ahlgren and K. Ono, Not. Am. Math. Soc. **48**, 978 (2001).
[29] P. Schattschneider, *Fundamentals of Inelastic Electron Scattering* (Springer, New York, 1986).
[30] P. Schattschneider and G. Sölkner, J. Microsc. **134**, 73 (1984).
[31] I. S. Tilinin and W. S. M. Werner, Phys. Rev. B **46**, 13 739 (1992).
[32] I. S. Tilinin, A. Jablonski, and W. S. M. Werner, Prog. Surf. Sci. **52**, 193 (1997).
[33] W. S. M. Werner, I. S. Tilinin, and A. Jablonski, Surf. Interface Anal. **23**, 823 (1995).
[34] S. Tanuma, C. J. Powell, and D. R. Penn, Surf. Interface Anal. **21**, 165 (1994).